

CFD INVESTIGATION OF EFFECT OF LARGE SCALE ROUGHNESS HEIGHT OVER AN AERODYNAMIC PROFILE

G. Sivaraj

E- Mail: gsr304@gmail.com
Department Of Mechanical Engineering,
Anna University Regional Campus,
Tirunelveli, India.

K. Karuppasamy

Department Of Mechanical Engineering,
Anna University Regional Campus,
Tirunelveli, India.

Abstract-The efficiency of an airplane wing is often degraded by flow separation. Flow separation on an airfoil profile is related to the aerodynamic design. The performance for mission in aircraft is achieved by either: (a) airfoil surface-flow control methods, or (b) varying the geometry of the airfoil for changing free stream conditions-adaptive wing technology. The objective of this project work is to increase the stall angle and delay the flow separation point over the airfoil. This project deals about the large scale roughness size effect over the airfoil profile and also will give an over view of the results that is obtained for increasing stall angle by the creation of large scale roughness. In this paper effect of large scale roughness on flow separation and its controls are discussed. This work aims at selection of an airfoil with improved aerodynamic characteristics by CFD optimization. The NACA4415 airfoil is modified with large scale roughness. The investigation is made by varying the height of the bump in the order of 1.5% of chord, 2% of chord and 2.5% of chord. From the CFD results the airfoil with a bump height of 2.5% of chord is marked as efficient with improved stall angle and the flow separation is found delayed with decrease in drag and lift is increased, comparing to NACA4415 airfoil. After the airfoil profile design generation and meshing, the performance calculation had been carried out to evaluate the aerodynamic coefficients for various angle of attack. The results obtained for airfoil with large scale roughness is compared with the airfoil without large scale roughness. The stall angle has increased from 17 to 23 by the creation of large scale roughness in an airfoil. The designing of the airfoil with a roughness and meshing is done by using GAMBIT. The analysis of fluid flow separation in an airfoil due to various sizes of large scale roughness and its effects on the aerodynamic efficiencies is carried out using FLUENT at a low velocity of 30m/s.

Key words: *Airfoil, Large scale roughness, protuberances, Angle of attack, Flow separation, Stalling angle, Bump surface.*

1. Introduction

The Subsonic aerodynamics, not a major area of study until the recent past, promises tremendous potential in the development of small, robust and high performance aircraft Unmanned Aerial Vehicles (UAVs), Remotely Piloted Vehicles (RPVs) and Micro Aerial Vehicles (MAVs) [4]. These are particularly useful for defence applications such as surveillance, communication links, ship decoys and detection of biological, chemical or nuclear materials. Another important application of these vehicles has been identified in space or planetary exploration, especially in extreme low density environments such as in Mars [2]. These vehicles present extreme constraints to the airfoil design process in the form of (a) extreme operating conditions (cruise velocity, altitude, density) and (b) very small aspect ratios. The mission profiles tend to incorporate entirely different regimes in terms of their speed, altitude and maneuvering requirements [7]. For example, RPVs need to be operative at both normal and very high altitudes (where the density of air is low). From a fluid dynamist's point of

view, the performance of an aircraft is essentially controlled by the development of the boundary layer on its surface and its interaction with the mean flow. This interaction decides the pressure distribution on the airfoil surface and subsequently the aerodynamic loads on the wing. In order to obtain the highest levels of performance efficiencies for mission varying aircraft, it is necessary to either: (a) alter the boundary layer behaviour over the airfoil surface—flow control methods of interest here, and/or (b) change the geometry of the airfoil real time for changing free stream conditions—adaptive wing technology [15]. The value of aerodynamic efficiency needs to be maximum i.e. the lift to the drag ratio needs to be maximized. For this case lift should be high and drag should be low. This paper discusses the cfd results of flow control method by changing the airfoil surface geometry to improve the performance of the airfoil as well as aircraft.

2. Methodology

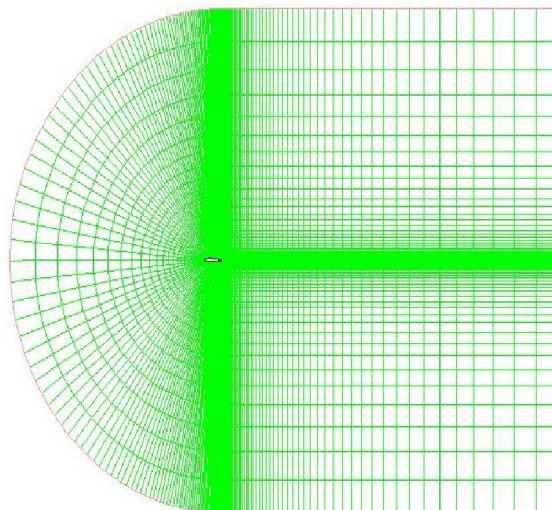
Aerodynamic analysis can be done either using conventional wind tunnel testing method. The wind tunnel testing is not convenient for frequent testing as well as time consuming, so we choose software analysis to test the model. The analysis is done using ANSYS 15.0 software. The model is subjected to lift analysis, drag analysis and velocity magnitude analysis.

The various pressure distribution such as static pressure, dynamic pressure, total pressure. Thus the above mentioned pressure distribution over the model is measured using CFD analysis. The following steps are done for the successful completion of analysis.

- i. Using GAMBIT software, Create the 2D model., Mesh the model., Create the named selections., Save the meshed model in *.msh format.
- ii. Using ANSYS software, CFD – FLUENT, Specify the fluid properties., Apply the boundary conditions., Initialize the solution., Specify iteration limit, Run calculation, At some iteration limit the solution will be converged, For viewing results, go to postprocessor and view results, The results are viewed as either contours or as vector plots.

2.1 Mesh Creation

The mesh creation is important step in the analysis. The dimensional structured quadrilateral mesh was utilized for computing flow around the model, because structured model is highly space efficient. Storage requirements for an unstructured mesh is substantially larger. The meshing is shown in figure 1. This meshing was done by using GAMBIT



Mesh

Nov 24, 2015
ANSYS Fluent 15.0 (2d, dp, pbns, lam)

Figure 1 Mesh model

2.2 Solver

Fluent solves the integral form of the governing equations for conservation of mass, momentum and energy and other scalars such as turbulence and chemical species when required using a finite volume discretization process. FLUENT allows for either a 2D or 3D CFD analysis, which is to be specified at startup. Also, FLUENT has 2 types of inbuilt solvers: pressure-based solver and density based solver. The pressure based solver was developed for low speed incompressible flows whereas the density-based solver was meant for high speed compressible flows. In both cases the velocity field is obtained by solving the momentum equations. In density-based approach, the continuity equation is used to acquire the density field and the pressure field is resolved from the equation of state. While in the pressure based approach, the pressure field is acquired by solving a pressure or pressure correction equation. Which is obtained by manipulating continuity and momentum equations. The numerical simulation by the solver was made after the completion of the mesh generation. The solver formulation of turbulence model spalart allmaras, boundary condition, solution control parameters and material properties were defined. After all the parameters were specified, the model was initialized. The initializing and iteration processes stopped after the completion of the computations. The results obtained were examined and analyzed.

3. Result And Discussion

3.1 Analysis Of Lift Coefficient (C_l)

Table 1 shows the lift coefficient changes with angle of attack, for Naca4415, 1.5% c bump and 2.5% c bump at velocity of 30 m/s

Table 1 Lift coefficient

S.NO	ANGLE OF ATTACK	NACA 4415	1.5% c bump	2.5% c bump
1	17	0.15996	0.13463	0.12746
2	19	0.15855	0.14410	0.14054
3	21	0.15105	0.15013	0.15272
4	23	0.14020	0.14792	0.16392

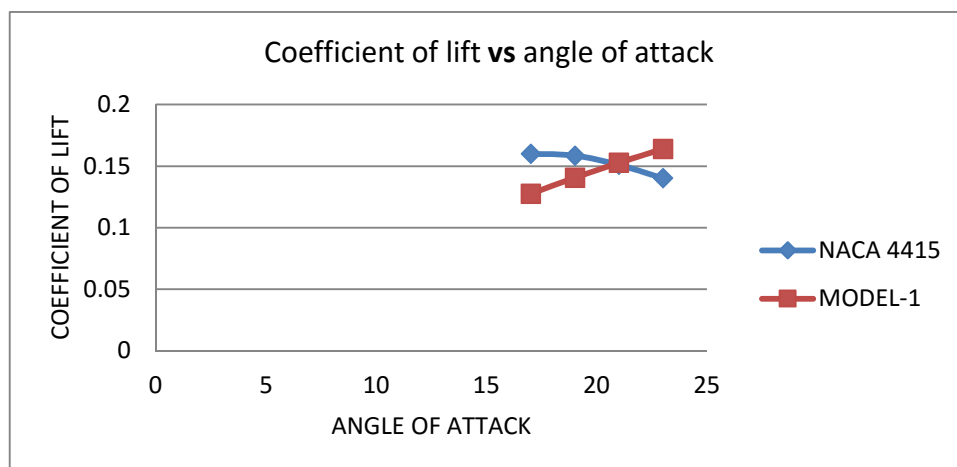


Figure 2 Lift coefficient vs angle of attack

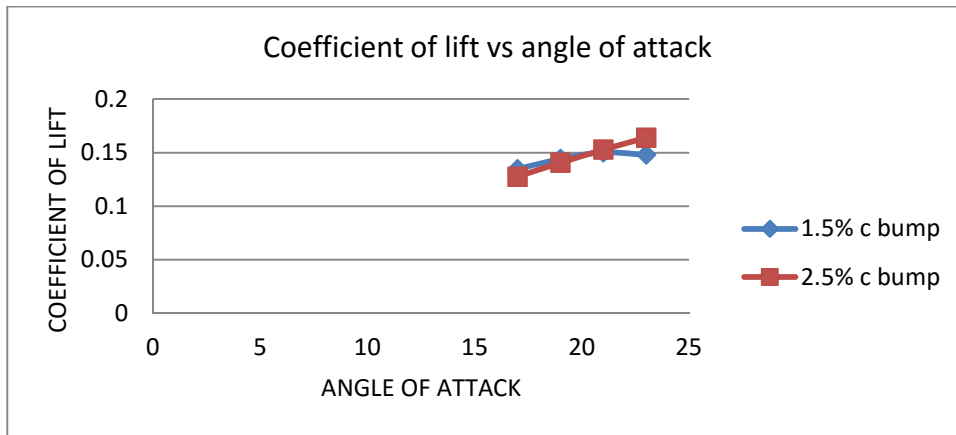


Figure 2.1 Lift coefficient vs angle of attack

From the above figure 2 and figure 2.1 it is observed that for high angle of attack the model with the bump height of 2.5%*c* is give the maximum lift coefficient comparing to the 1.5%*c* bump model as well as naca4415 model.

3.2 Analysis Of Drag Coefficient (*C_d*)

Table 2 shows the drag coefficient changes with angle of attack, for Naca4415, 1.5% *c* bump and 2.5% *c* bump at velocity of 30 m/s

Table 2 Drag coefficient

S.NO	ANGLE OF ATTACK	NACA 4415	1.5% c bump	2.5% c bump
1	17	0.02474	0.02363	0.02353
2	19	0.02823	0.02733	0.02721
3	21	0.03168	0.03118	0.03106
4	23	0.03537	0.03503	0.03512

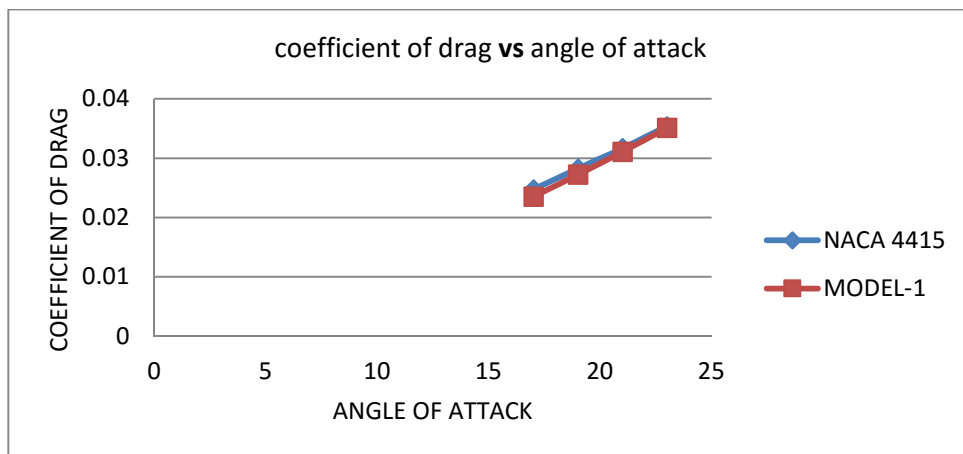


Figure 3 Drag coefficient vs angle of attack

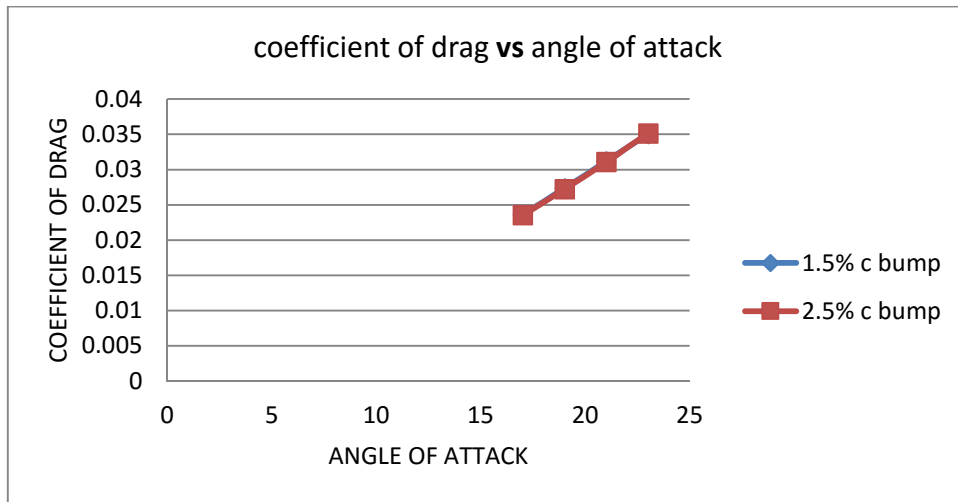


Figure 3.1 Drag coefficient vs angle of attack

From the above figure 3 and figure 3.1 it is observed that for high angle of attack the model with the bump height of 2.5%c and the 1.5%c bump model gives more or less equal drag coefficient value as well as naca4415 model gives higher drag coefficient value.

3.3 Static Pressure Contours

The pressure which is experienced by an object in flow only due to the random motion of gas molecules hitting the surface of the body. The static pressure of a flow decreases with velocity and altitude as well.

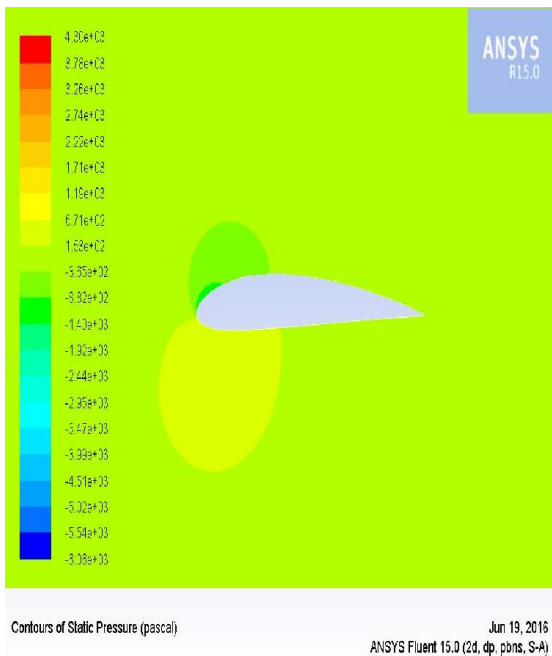


Figure 4. Naca 4415 model

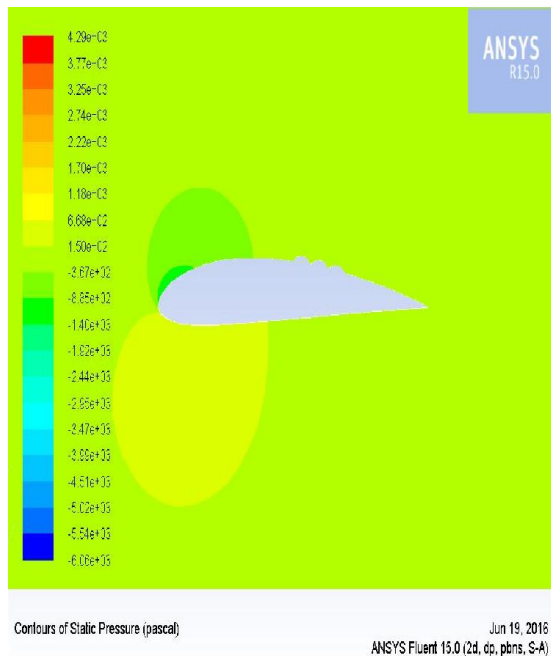


Figure 4.1 1.5% c bump model

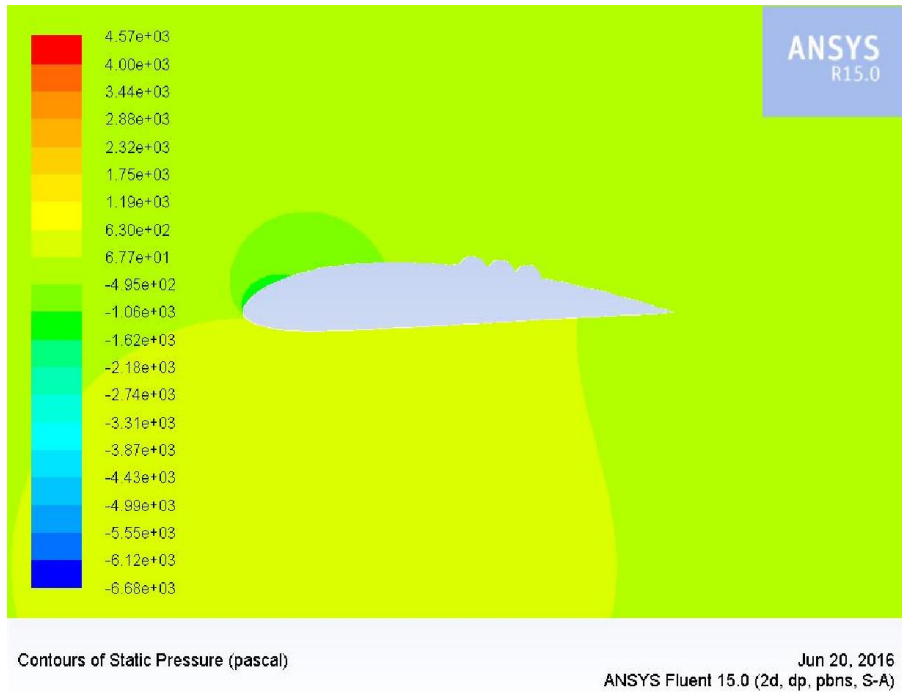


Figure 4.2. 2.5% c bump model

The static pressure of a flow decreases with velocity and altitude as well. Figure 4, figure 4.1 and figure 4.2 shows a combination of the static pressure over the wall i.e. airfoil surface for each case at angle of attack, $\alpha=23^\circ$

3.4 Dynamic Pressure Contours

The pressure of the flow associated with the velocity of the flow or by virtue of velocity. Hence, by definition the dynamic pressure will be high in the flow field where the velocity is high and vice versa.

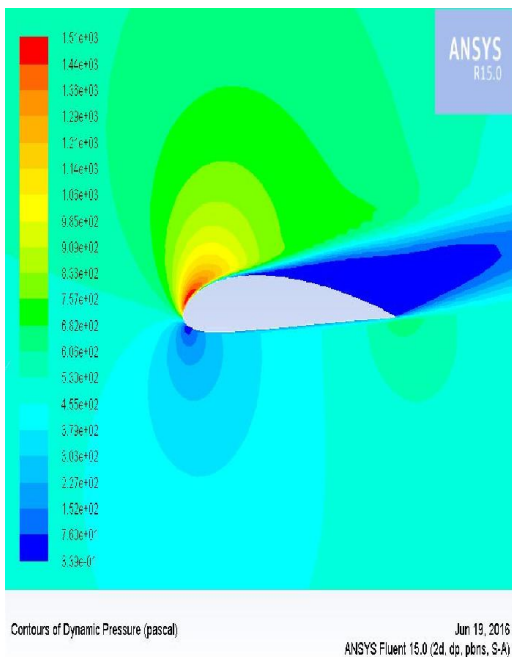


Figure 5 Naca 4415 model

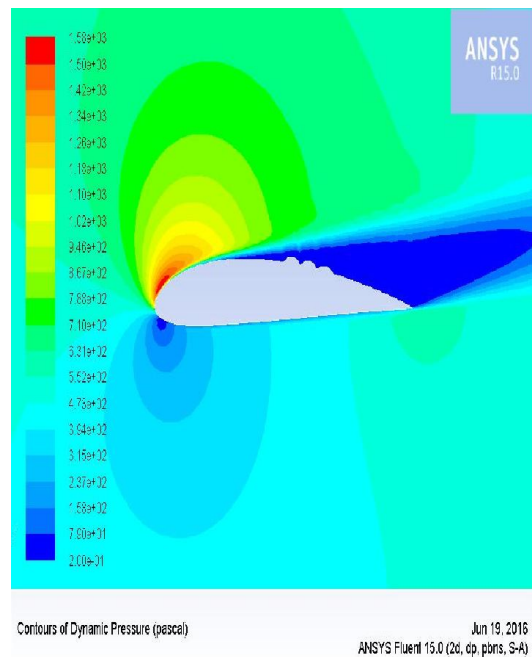


Figure 5.1 1.5% c bump model

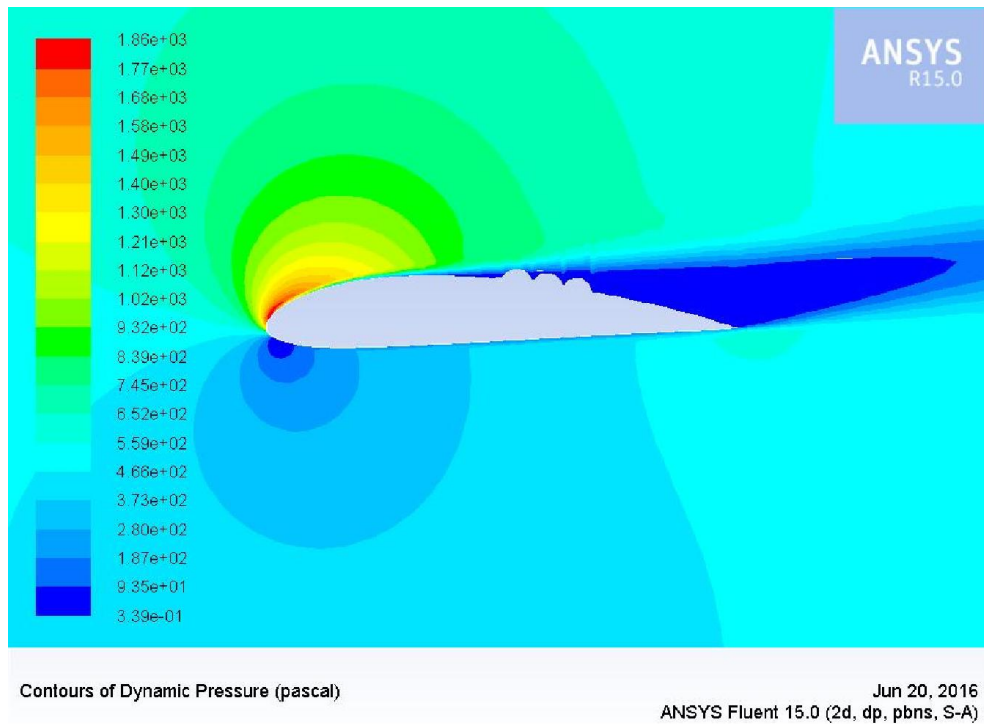


Figure 5.2 2.5% c bump model

Figure 5, figure 5.1 and figure 5.2 shows a combination of dynamic pressure contours over the wall i.e. airfoil surface for each case at angle of attack, $\alpha=23^\circ$

3.5 Lift Convergence

The lift coefficient is also a dimensionless quantity that indicates the degree of lift, the pressure and viscous force that acts in the direction opposite to the motion of the body through the flow, opposing its downward motion. The lift coefficient is also a function of angle of attack and Reynolds number of the flow.

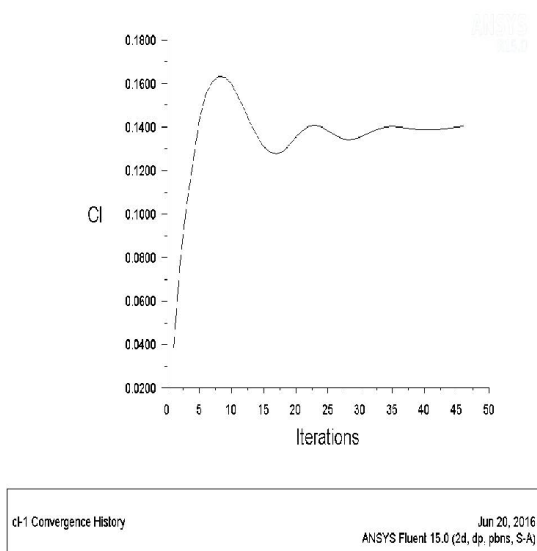


Figure 6 Naca 4415 model

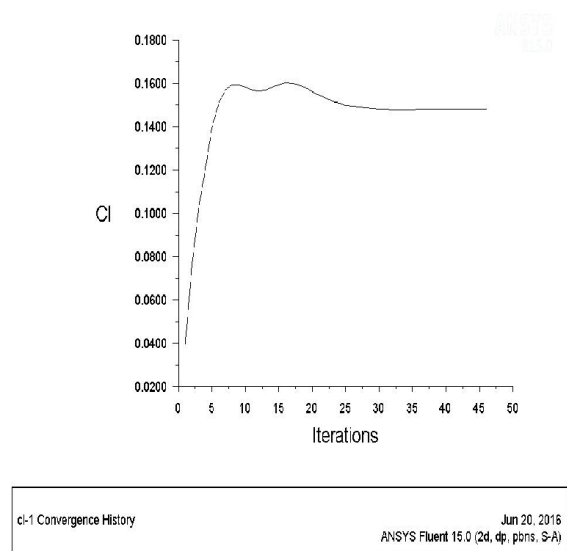


Figure 6.1 1.5% c bump model

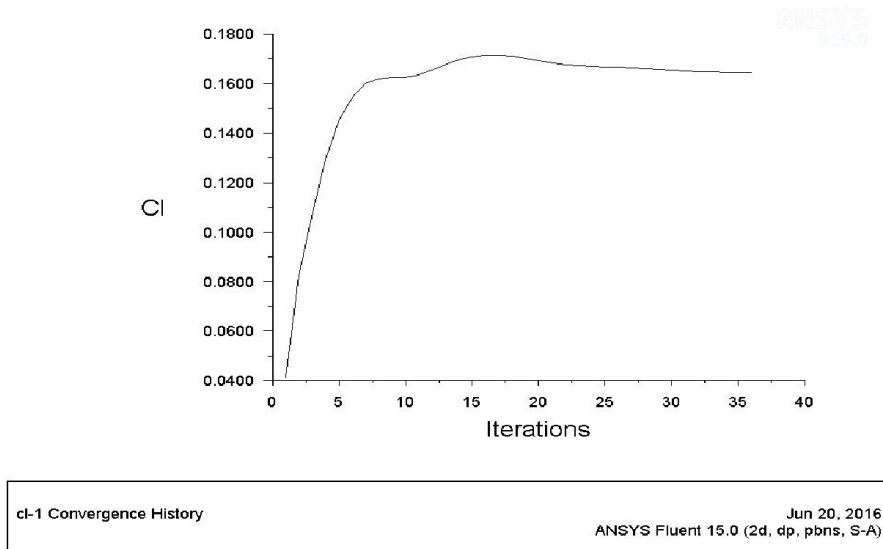


Figure 6.2 2.5% c bump mode

Lift convergence is shown in figure 6, figure 6.1 and figure 6.2 for angle of attack, $\alpha=23^\circ$. From that it is observed that for high angle of attack the model with the bump height of 2.5%c is give the maximum lift comparing to the 1.5%c bump model as well as naca4415 model.

3.6 Drag convergence

The drag coefficient is also a dimensionless quantity that indicates the degree of drag, the pressure and viscous force that acts in the direction opposite to the motion of the body through the flow, opposing its forward motion. The drag coefficient is also a function of angle of attack and Reynolds number of the flow. Drag convergence is shown in figure for angle of attack, $\alpha=23^\circ$

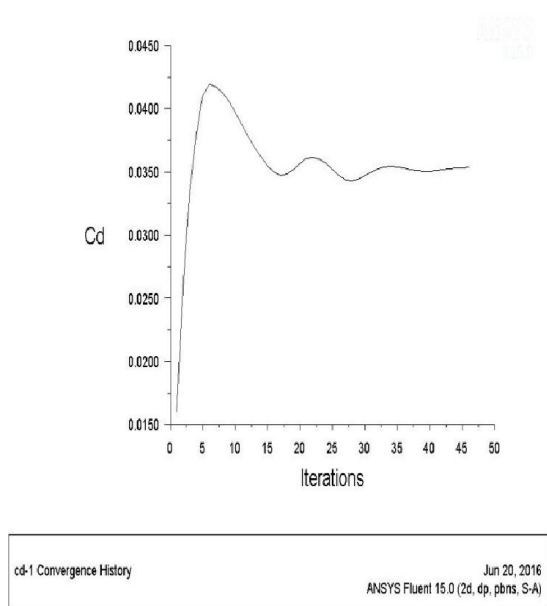


Figure 7 Naca 4415 model

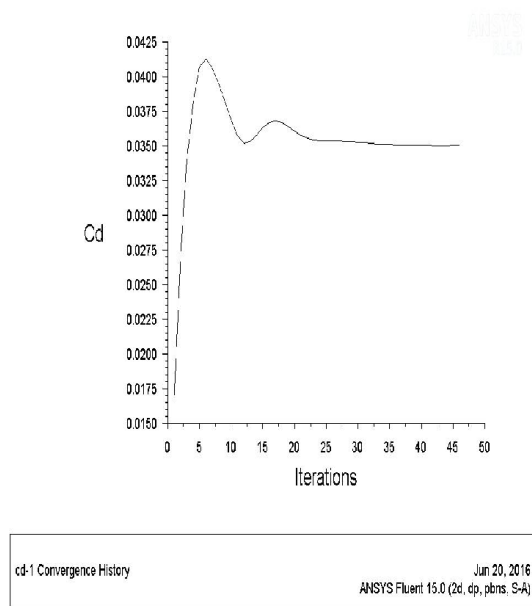


Figure 7.1 1.5% c bump model

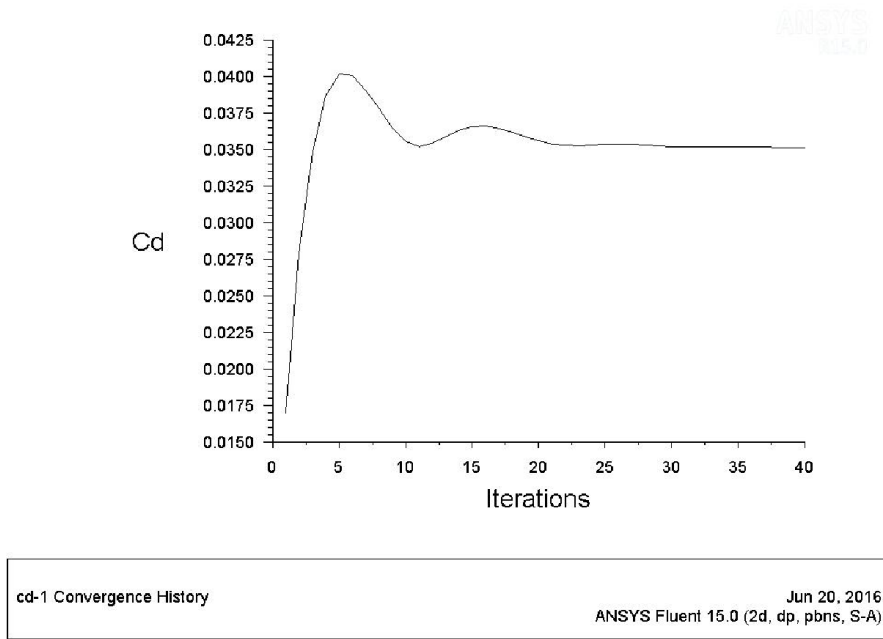


Figure 7.2 2.5% c bump model

Drag convergence is shown in figure 7, figure 7.1 and figure 7.2 for angle of attack, $\alpha=23^\circ$. From that it is observed that for high angle of attack the model with the bump height of 2.5%c and the 1.5%c bump model gives more or less equal drag value as well as naca4415 model gives higher drag value.

3.7 Pathlines

From the comparison of pathlines for Naca 4415 without roughness and models with roughness, show the boundary layer separation. By extending the separation point we can increase the lift of the wing and can obtain the better performance.

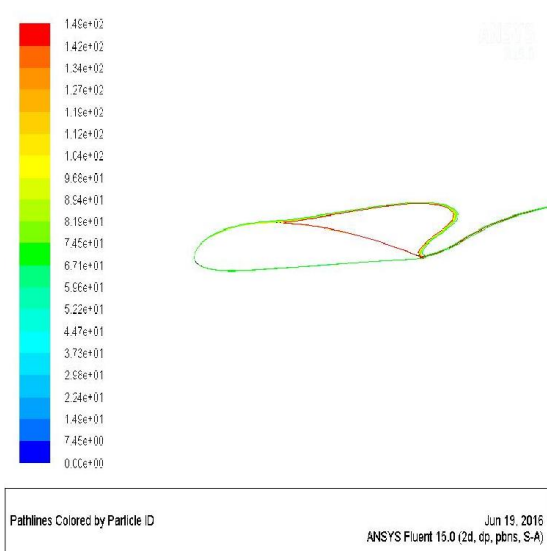


Figure 8 Naca 4415 model

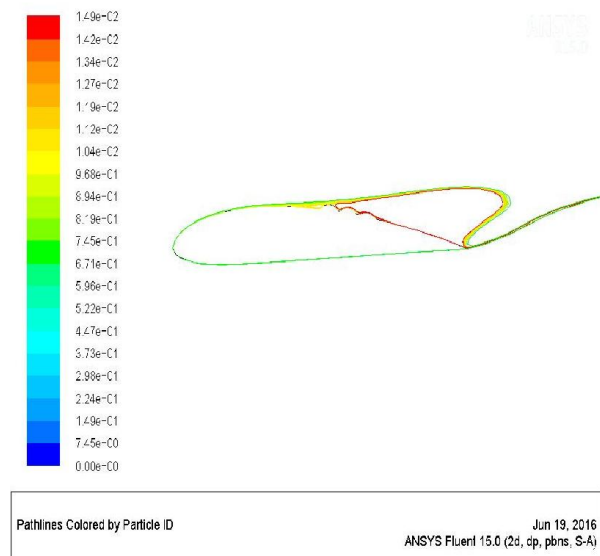


Figure 8.1 1.5% c bump model

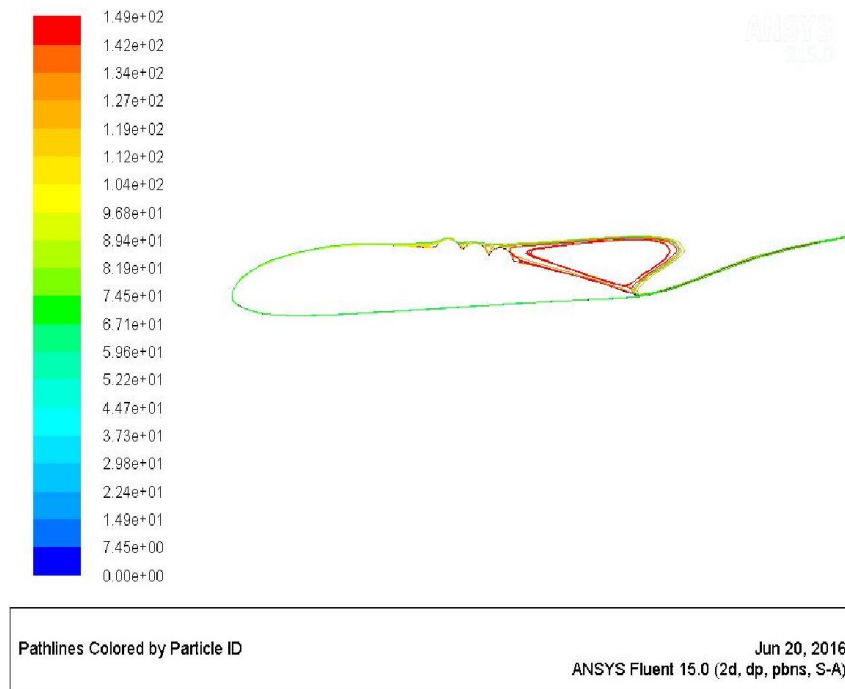


Figure 8.2 2.5% c bump model

Pathlines is shown in figure 8, figure 8.1 and figure 8.2 for angle of attack, $\alpha=23^\circ$. From that it is observed that the model with the bump height of 2.5%c is efficient and capable to re attach the flow at high angle of attacks comparing to the 1.5%c bump model and naca4415 model.

The result from the 2dimensional airfoil with bump model was compared to the 2-dimensional airfoil without bump. The discussions were focused on the aerodynamics characteristics which include drag coefficient CD, lift coefficient CL. In addition, the pressure contours and path lines is also observed. The simulation was carried out at various angles of attack, NACA airfoil 4415 it stalled at 17 degree angle of attack. Thus, simulation was done between 17 and 23 degree angles of attack at 30 m/s velocity.

4. Future Enhancement And Conclusion

4.1 Future Recommendation

The lift coefficient is increased by using this bump concept. the bump height in the order of 2.5% chord length is effective to reattach the flow comparing to the bump height in the order of 1.5% chord length. For obtaining the best result and know the effects on aerodynamic characteristic of bump, we can analyse the model with fully bumpy model at various speed. The investigation can be done at high Reynolds number to know the relationship between them because flow type depends Reynolds number. We can change the number of bumps, locations and dimensions of bump and can do the same experiment. If we use different flow solver then the accuracy of result can be checked to know the lift increment by the creation bumps on suction side of airfoil.

4.2 Limitation

Bump size and location should be considered.

Bump height must be in appropriate height. Should not be less than 2.5% chord length and greater than 2.5% chord length otherwise it will be ineffective.

4.3 Conclusion

The bump surface at certain location over the upper camber of airfoil, results to increase in the stall angle. The bump height in the order of 2.5% chord length have given better performance than the without bump case. From that we can know that the height of bumps plays an important role, the bump in an ineffective height will give negative results only.. The stall angle of NACA 4415 airfoil is 17 degree but 23 degree for the airfoil with bump height of 2.5% chord length and the lift increment is obtained because at stall angle or high angle of attack the bump can reattach the flow where the flow separation starts. So it will increase the lift and increase the stall angle. From this cfd investigation it has been observed that the flow separation on the surface of the airfoil can be delayed by the modification with regular perturbations or “bumps”. It was found that the stall angle was delayed, when compared to the “smooth” baseline case, with increase in lift and decrease in drag. The lift of bumps surface airfoil will be greater than the smooth surface. This also implies that the bumpy surface improves the aerodynamic characteristics of the wing for low Re flow

References

1. Shan. H, Li Jiang, Chaoqun (2005) ‘Direct Numerical Simulation Of Flow Separation Around A Naca 0012 Airfoil’ *Computers & Fluids* Vol. 34, pp. 1096–1114.
2. Jianliang. W, Ji Yao, Weibin Yuan, Huimin Wang, Liang Cao (2012) ‘Analysis On The Influence Of Turbulence Model Changes To Aerodynamic Performance Of Vertical Axis Wind Turbine’ *Procedia Engineering* Vol. 31, pp. 274 – 281.
3. Ribeiro. A.F.P, A.M. Awruch, H.M. Gomes (2012) ‘An Airfoil Optimization Technique For Wind Turbines’ *Applied Mathematical Modelling* Vol. 36, pp. 4898–4907.
4. Tomoaki. I, Takashiatobe, Shoheitakagi (2012) ‘Direct Simulations Of Trailing-Edge Noise Generation From Two-Dimensional Airfoils At Low Reynolds Numbers’ *Journal Of Sound And Vibration* Vol. 331, pp. 556–574.
5. Yao. J, Weibin Yuan, Jianliang Wang, Jianbin Xie , Haipeng Zhou, Mingjun Peng, Yong Sun (2012) ‘Numerical Simulation Of Aerodynamic Performance For Two Dimensional Wind Turbine Airfoils’ *Procedia Engineering* Vol. 31, pp. 80 – 86.
6. Gim. O.S, Gyoung-Woolee (2013) ‘Flow Characteristics And Tip Vortex Formation Around A Naca 0018 Foil With An Endplate’ *Ocean Engineering* Vol. 60, pp. 28–38.
7. Hinz. D.F, Hekmat Alighanbari, Christian Breitsamter (2013) ‘Influence Of Heat Transfer On The Aerodynamic Performance Of A Plunging And Pitching Naca0012 Airfoil At Low Reynolds Numbers’ *Journal Of Fluids And Structures* Vol. 37, pp. 88–99.
8. Lehmkuhl. O, I. Rodríguez, A. Baez, A. Oliva, C.D. Pérez-Segarra (2013) ‘On The Large-Eddy Simulations For The Flow Around Aerodynamic Profiles Using Unstructured Grids’ *Computers & Fluids* Vol. 84, pp. 176–189.
9. Mudunkotuwe. H.V.D.Y.M, Kato Chisachi (2013) ‘Large Eddy Simulations Of 2d And Open-Tip Airfoils Using Voxel Meshes’ *Procedia Engineering* Vol. 61, pp. 32 – 39.
10. Rodriguez, O. Lehmkuhl, R. Borrell, A. Oliva (2013) ‘Direct Numerical Simulation Of A Naca0012 In Full Stall’ *International Journal Of Heat And Fluid Flow* Vol. 43, pp. 194–203.
11. Sengupta. T.K, Ashish Bhole, N.A. Sreejith (2013) ‘Direct Numerical Simulation Of 2d Transonic Flows Around Airfoils’ *Computers & Fluids* Vol. 88, pp. 19–37.
12. Bai. T, Jingyuan Liu, Weihao Zhang, Zhengping Zou (2014) ‘Effect Of Surface Roughness On The Aerodynamic Performance Of Turbine Blade Cascade’ *Propulsion And Power Research* Vol. 3 No. 2, pp. 82–89.

13. Charan D.P, Devi Prasad Mishra (2014) 'CFD Simulations For The Selection Of An Appropriate Blade Profile For Improving Energy Efficiency In Axial Flow Mine Ventilation Fans' Journal Of Sustainable Mining E-Issn 2300-3960, P-Issn 2300-1364.
14. Cheng. L.Z, Xue Lei-Ping (2014) 'Detached-Eddy Simulation Of Wing-Tip Vortex In The Near Field Of Naca 0015 Airfoil' Journal Of Hydrodynamics, Vol. 26 No. 2, pp. 199-206.
15. Faruqui. S.H.A, Md. Abdullah Albari, Mdemran, Ahsan Ferdaus (2014) 'Numerical Analysis Of Role Of Bumpy Surface To Control The Flow Separation Of An Airfoil' Procedia Engineering Vol. 90, pp. 255 – 260.
16. Qiulinqu, Xijia, Weiwang, Peiqingliu, Ramesh K.Agarwal (2014) 'Numerical Study Of The Aerodynamics Of A Naca 4412 Airfoil In Dynamic Ground Effect' Aerospace Science And Technology.
17. Sani. A.S, Ehsan Roohi, Mohsen Kahroma, Stefan Stefanov, (2014) 'Investigation Of Aerodynamic Characteristics Of Rarefied Flow Around Naca 0012 Airfoil Using Dsmc And Ns Solvers' European Journal Of Mechanics B/Fluids Vol. 48, pp. 59–74.
18. Wang. L, Liying Li, Song Fu (2014) 'Numerical Investigation Of Active Flow Control On A Pitching Naca 0015 Airfoil Using Detached-Eddy Simulation' Procedia Engineering Vol. 79, pp. 49 – 54.
19. Azim. R, M. M. Hasan And Mohammad Ali (2015) 'Numerical Investigation On The Delay Of Boundary Layer Separation By Suction For Naca 4412' Procedia Engineering Vol. 105, pp. 329 – 334.
20. Hefeng. D, Wang Chenxi, Li Shaobin, Song Xi Zhen (2015) 'Numerical Research On Segmented Flexible Airfoils Considering Fluid-Structure Interaction' Procedia Engineering Vol. 99, pp. 57 – 66.